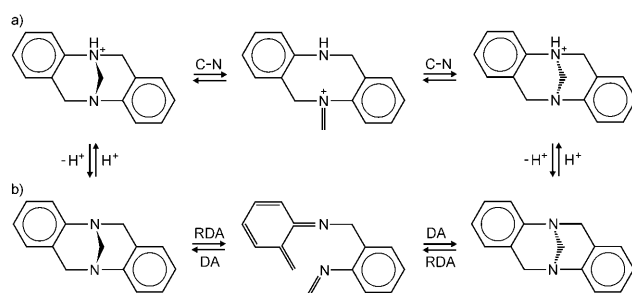


# In-Flight Epimerization of a Bis-Tröger Base\*\*

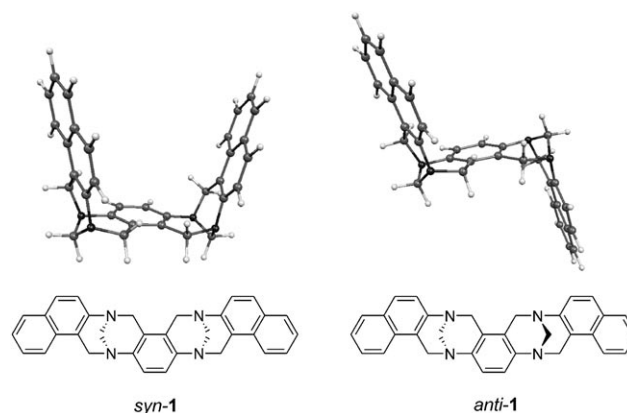
Ágnes Révész, Detlef Schröder,\* Tibor András Rokob, Martin Havlík, and Bohumil Dolenský

In 1887, Julius Tröger reported the synthesis of a nitrogen base,<sup>[1]</sup> whose structure was determined only about 50 years later.<sup>[2]</sup> In “Tröger bases”, nitrogen atoms serve as chiral centers because the otherwise rapid nitrogen inversion is prevented by conformational strain. After Prelog and Wieland separated the enantiomers,<sup>[3]</sup> the chirality and the rigid V-shape of Tröger bases led to widespread applications in chemistry.<sup>[4]</sup> A fundamental question in the chemistry of Tröger bases concerns the mechanism of their pseudo-epimerization,<sup>[5]</sup> for which either a proton-catalyzed ring opening or a retro-Diels–Alder (RDA) sequence has been proposed (Scheme 1).<sup>[6]</sup>



**Scheme 1.** Proposed pseudo-epimerization mechanisms of Tröger bases proceeding by a) proton-catalyzed ring opening and b) an RDA sequence.

Herein, we report studies of the bis-Tröger bases *syn*-**1** and *anti*-**1** (Scheme 2)<sup>[7,8]</sup> using ion-mobility mass spectrometry (IM-MS), a mass-spectrometric method that distinguishes ionic species not only by mass, but also in terms of shape.<sup>[9–11]</sup> Provided a separation of *syn*-**1** and *anti*-**1** by means of IM-MS, the epimerization in the gaseous state may be probed directly, because for **1** this process leads from one diastereoisomer to another.<sup>[12]</sup>



**Scheme 2.** Bis-Tröger bases *syn*-**1** and *anti*-**1**. The structures shown correspond to the lowest energy conformers according to density functional theory.

We first considered the protonated species *syn*-**1**H<sup>+</sup> and *anti*-**1**H<sup>+</sup> formed by electrospray ionization (ESI).<sup>[13]</sup> Both diastereoisomeric samples show two, well-separated components in the ion-mobility traces of the protonated ions. *syn*-**1** gives a large signal at an early arrival time  $t_a = 6.8$  ms<sup>[14]</sup> and a smaller signal at  $t_a = 7.4$  ms (Figure 1 a). In contrast, *anti*-**1** has

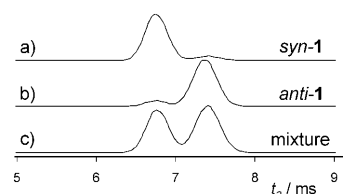


**Figure 1.** Ion-mobility traces of the mass-selected protonated ions ( $m/z$  467) for a) *syn*-**1**, b) *anti*-**1**, and c) a roughly 1:1 mixture of the two samples as a control.

large signal at later arrival time and a small signal for the early component (Figure 1 b). Since *syn*-**1** and *anti*-**1** were diastereomerically pure (according to their NMR spectra), the small components are attributed to partial isomerization during ESI (see below).

To induce an interconversion between the diastereoisomers, we pursued two different strategies. In ESI, a liquid sample is sprayed to the inlet system of a mass spectrometer. Ionic species, either present as such in solution or formed in the spray process by microscopic fluctuations, are subsequently desolvated and transferred to the mass spectrometer.<sup>[15]</sup> In ESI no “hard” ionization event is applied, such that the molecules present in solution are typically transferred to the gas phase as molecular or quasi-molecular ions.<sup>[16]</sup>

[\*] Á. Révész, Dr. D. Schröder, Dr. T. A. Rokob  
 Institute of Organic Chemistry and Biochemistry  
 Flemingovo náměstí 2, 16610 Prague 6 (Czech Republic)  
 Fax: (+420) 220-183-462  
 E-mail: schroeder@uochb.cas.cz

Dr. M. Havlík, Dr. B. Dolenský  
 Department of Analytical Chemistry  
 Institute of Chemical Technology Prague  
 Technická 5, 16628 Prague 6 (Czech Republic)

[\*\*] This work was supported by the Academy of Sciences of the Czech Republic (Z40550506), the European Research Council (AdG HORIZOMS), the Grant Agency of the Czech Republic (203/08/1445), and the Ministry of Education, Youth and Sports of the Czech Republic (MSM 6046137307 and LC 521).

Supporting information for this article is available on the WWW under <http://dx.doi.org/10.1002/anie.201007162>.

However, the actual conditions within the ESI source can be varied over a rather wide range such that either weakly bound noncovalent complexes are generated<sup>[17]</sup> or the ions are energized to afford isomerization<sup>[18]</sup> as well as dissociation.<sup>[19]</sup> Adjusting the ionization conditions to higher energies can easily be achieved by increase of the so-called cone voltage ( $U_c$ )<sup>[20]</sup> which is used to extract the ions into the mass spectrometer. At elevated cone voltages, the ions undergo multiple collisions with nitrogen (1 bar) which increase their internal energy. Figure 2 shows such experiments for  $1H^+$  generated at different cone voltages from which two conclusions can be drawn: 1) Energizing collisions lead to interconversions of *syn-1H*<sup>+</sup> and *anti-1H*<sup>+</sup>. 2) The amount of isomerization is somewhat lower for *anti-1H*<sup>+</sup>, suggesting it is the thermochemically preferred isomer.

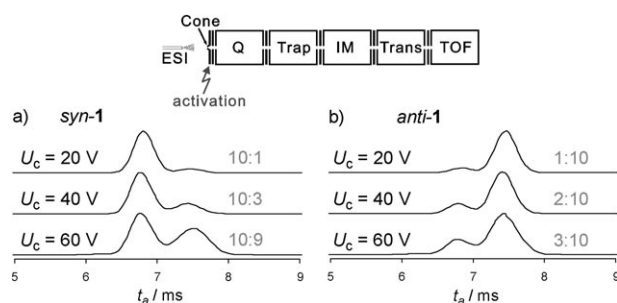


**Figure 2.** Ion-mobility traces of the mass-selected protonated ions ( $m/z$  467) generated from a) *syn-1* and b) *anti-1* at different cone voltages ( $U_c$ ) in the ESI source. The larger  $U_c$ , the more the ions are heated in multiple collisions. The gray numbers are the ratios of the integrated areas of the fast (early) and slow (late) components of  $1H^+$  at each  $U_c$ . The upper sketch of the IM-MS highlights where activation takes place (for details, see Ref. [10]).

The second method to induce isomerization also applies collisional activation, but now this step takes place in vacuum ( $10^{-2}$  mbar). Specifically, *syn-1H*<sup>+</sup> and *anti-1H*<sup>+</sup> generated at low cone voltages were subjected to collisional activation in the ion trap which collects the ions before they enter the IM stage.<sup>[21]</sup> Figure 3 demonstrates that the pseudo-epimerization

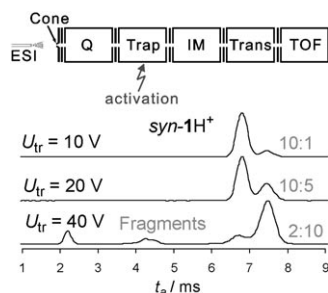


**Figure 3.** Ion-mobility traces of *syn-1H*<sup>+</sup> ( $m/z$  467,  $U_c$  = 20 V) at different voltages ( $U_{tr}$ ) applied to the ion trap in front of the ion-mobility device. The larger  $U_{tr}$ , the more the ions are heated in multiple collisions and also undergo fragmentation, but isomerization apparently starts to occur prior to dissociation. The gray numbers are the ratio of the integrated areas of the fast (early) and slow (late) components of  $1H^+$  at each  $U_{tr}$ .

can also be induced under these conditions by variation of the voltage setting of the trap ( $U_{tr}$ ). The consistent findings provide a direct link between collisional activation at 1 bar with that at  $10^{-2}$  mbar.

Figure 4 shows the ion-mobility spectrum of an approximately 1:1 mixture of *syn-1H*<sup>+</sup> and *anti-1H*<sup>+</sup>, the corresponding mass spectra upon collision-induced dissociation (CID)

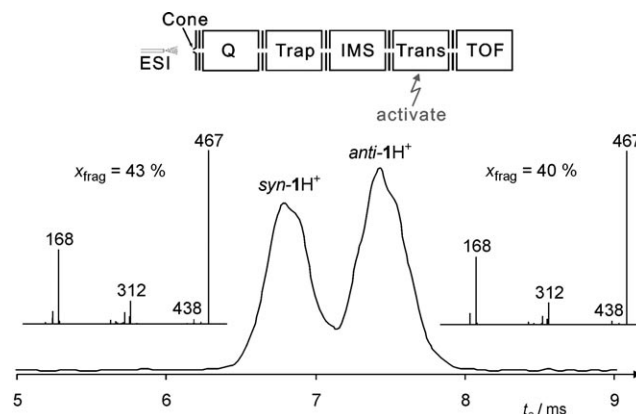


**Figure 4.** Ion-mobility trace of the protonated ions  $1H^+$  ( $m/z$  467,  $U_c$  = 20 V) generated from a roughly 1:1 mixture of *syn-1* and *anti-1*, and the CID mass spectra of the fast and the slow components.

after the ion-mobility section are shown in the insets. While the fragment ions formed and their ratios are identical for the two isomers, the total amount of fragmentation shows a slight, but significant difference. Thus, under perfectly identical conditions about  $x_{frag} = 43\%$ <sup>[22]</sup> of *syn-1H*<sup>+</sup> dissociates, whereas this fraction is only 40% for *anti-1H*<sup>+</sup>, again suggesting that the latter ion is slightly more stable than the *syn* isomer.

The conclusions derived from experiment were further supported by calculations using density functional theory.<sup>[23]</sup> For the neutral compounds, *anti-1* is predicted to be 1.5 kJ mol<sup>-1</sup> more stable than isomeric *syn-1*. For  $1H^+$ , protonation at nitrogen is highly preferred and both stereoisomers are energetically very close with the *anti* isomer being predicted to be 2.0 kJ mol<sup>-1</sup> more stable.<sup>[24]</sup>

Next, we considered the sodium adducts *syn-1Na*<sup>+</sup> and *anti-1Na*<sup>+</sup>. The change of the cationizing species has two important effects. At first, protonation of a base B is often understood in Brønsted terms in that a free proton is attached to B. But this is a rather formal view that neglects the pronounced covalent character of the new H–B bond, in that most of the positive charge is located in B rather than on the hydrogen atom.<sup>[25]</sup> In marked contrast, the sodiated species can be regarded as purely electrostatic adducts of Na<sup>+</sup> with B. The sodiated Tröger bases accordingly serve as gas-phase models for the neutral bases which are charge tagged by sodium to enable mass-spectrometric handling and detection.<sup>[26]</sup> If the pseudo-epimerization described above is an inherent feature of the backbone of the Tröger base regardless of the actual charge state (e.g. by RDA), it should occur for both  $1H^+$  and  $1Na^+$ , whereas in the case of proton catalysis, only  $1H^+$  should undergo isomerization. The second

effect is that since the radius of  $\text{Na}^+$  is larger than that of  $\text{H}^+$ , the additional (empty) valence orbitals available open up new kinds of coordination geometries.

Quite interestingly, the separation of *syn*- $\mathbf{1Na}^+$  and *anti*- $\mathbf{1Na}^+$  by IM-MS is much better than that of the protonated variants, and despite their slightly larger masses the sodiated ions have higher mobilities than the protonated forms (Figure 5). We note in passing that the ion-mobility traces

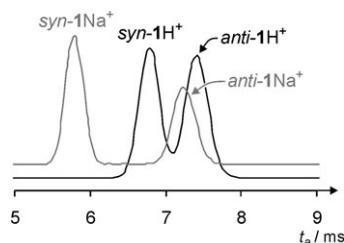


**Figure 5.** Mobility spectra of roughly 1:1 mixtures of *syn*- $\mathbf{1}$  and *anti*- $\mathbf{1}$  for the mass-selected protonated ions  $\mathbf{1H}^+$  ( $m/z$  467, black line) and the mass-selected sodiated species  $\mathbf{1Na}^+$  ( $m/z$  489, gray line); the latter were formed by admixture of one equivalent of  $\text{Na}_2\text{SO}_4$ .

of the diastereomeric samples show only very small contributions of the other diastereoisomer (<2%), such that the corresponding signals observed for  $\mathbf{1H}^+$  at lowest cone voltages (Figure 1) can already be assigned to a proton-catalyzed epimerization in the spray process.

Computational chemistry<sup>[23]</sup> provides a straightforward explanation of the pronounced differences between  $\mathbf{1H}^+$  and  $\mathbf{1Na}^+$ . Firstly, for  $\text{Na}^+$ , coordination to the  $\pi$  system of the aromatic rings is largely preferred over coordination to the nitrogen atoms. Secondly, in the case of *syn*- $\mathbf{1Na}^+$ , the metal cation interacts with the central benzene ring and the aromatic residues on both sides of the molecule leading to a rather compact geometry. In *anti*- $\mathbf{1Na}^+$ , a similar but much less pronounced effect is operative owing to coordination with an outer naphthalene unit and the central benzene ring. Given these pronounced differences in coordination geometry, it is not surprising that the cage structure *syn*- $\mathbf{1Na}^+$  is computed to be  $39.8 \text{ kJ mol}^{-1}$  more stable than *anti*- $\mathbf{1Na}^+$ .

As a result of chelation, the sodiated species are more compact than their protonated variants, which accounts for their higher mobilities. As demonstrated by the overlay of the optimized structures in Figure 6, this difference is small between *anti*- $\mathbf{1H}^+$  and *anti*- $\mathbf{1Na}^+$ , but much greater between *syn*- $\mathbf{1H}^+$  and *syn*- $\mathbf{1Na}^+$ . This result perfectly matches the experimental finding that the difference between the arrival times of *syn*- $\mathbf{1H}^+$  and *syn*- $\mathbf{1Na}^+$  ( $\Delta t_a = 1.0 \text{ ms}$ ) is much greater than between *anti*- $\mathbf{1H}^+$  and *anti*- $\mathbf{1Na}^+$  ( $\Delta t_a = 0.2 \text{ ms}$ ).

Finally, the sodiated species do not show any evidence of isomerization upon collisional activation either in the source region by means of the cone voltage nor in the ion trap preceding the ion-mobility cell (see the Supporting Information). If an RDA sequence were a viable alternative mechanism for pseudo-epimerization, it should also occur for the sodiated species. The absence of this process thereby suggests a proton-catalyzed ring-opening sequence as the

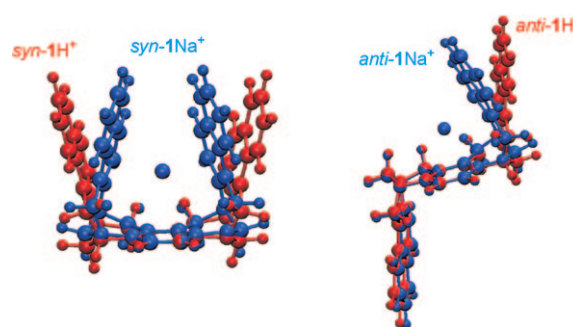


**Figure 6.** Overlay of the structures of *syn*- $\mathbf{1H}^+$  and *syn*- $\mathbf{1Na}^+$  (left) and of *anti*- $\mathbf{1H}^+$  and *anti*- $\mathbf{1Na}^+$  (right).

more probable mechanism for the isomerization of Tröger bases.

In addition to the implications for the chemistry of Tröger bases, the present study demonstrates the useful chemical insight provided by ion-mobility mass spectrometry. Moreover, by parallel monitoring of the isomerization in the source region with atmospheric pressure and in the dilute vacuum of the collision cell, this work contributes to bridging the “pressure gap”<sup>[27]</sup> between idealized studies in the gas phase and real chemistry in the bulk.

Received: November 15, 2010

Published online: February 8, 2011

**Keywords:** aggregation · epimerization · ion-mobility mass spectrometry · sodium complexes · Tröger bases

- [1] J. Tröger, *J. Prakt. Chem.* **1887**, 36, 225–245.
- [2] M. A. Spielman, *J. Am. Chem. Soc.* **1935**, 57, 583–585.
- [3] V. Prelog, P. Wieland, *Helv. Chim. Acta* **1944**, 27, 1127–1134.
- [4] a) B. G. Bag, *Curr. Sci.* **1995**, 68, 279–288; b) M. Valík, R. M. Strongin, V. Král, *Supramol. Chem.* **2005**, 17, 347–367; c) B. Dolenský, J. Elguero, V. Král, C. Pardo, M. Valík, *Adv. Heterocycl. Chem.* **2007**, 93, 1–56; d) S. Sergeyev, *Helv. Chim. Acta* **2009**, 92, 415–444; e) T. Weilandt, U. Kiehne, J. Bunzen, G. Schnakenburg, A. Lützen, *Chem. Eur. J.* **2010**, 16, 2418–2426.
- [5] According to the IUPAC definition, the interconversion of the two enantiomers is not a true epimerization because two stereocenters change configuration, see: <http://goldbook.iupac.org/E02167.html>.
- [6] a) A. Greenberg, N. Molinaro, M. Lang, *J. Org. Chem.* **1984**, 49, 1127–1130; b) O. Trapp, V. Schurig, *J. Am. Chem. Soc.* **2000**, 122, 1424–1430; c) D. A. Lenev, K. A. Lyssenko, D. G. Golovanov, V. Buss, R. G. Kostyanovsky, *Chem. Eur. J.* **2006**, 12, 6412–6418; d) O. Trapp, G. Trapp, J. Kong, U. Hahn, F. Vögtle, V. Schurig, *Chem. Eur. J.* **2002**, 8, 3629–3634; e) J. Artacho, P. Nilsson, K.-E. Bergquist, O. F. Wendt, K. Wärnmark, *Chem. Eur. J.* **2006**, 12, 2692–2701.
- [7] a) C. Pardo, E. Sesmi, E. Gutierrez-Puebla, A. Monge, J. Elguero, A. Fruchier, *J. Org. Chem.* **2001**, 66, 1607–1611; b) T. Mas, C. Pardo, F. Salort, J. Elguero, R. M. Torres, *Eur. J. Org. Chem.* **2004**, 1097–1104.
- [8] a) M. Valík, B. Dolenský, H. Petříčková, V. Král, *Collect. Czech. Chem. Commun.* **2002**, 67, 609–621; b) M. Havlík, V. Král, B. Dolenský, *Org. Lett.* **2006**, 8, 4867–4870; c) B. Dolenský, M.

Valík, P. Matějka, E. Herdtweck, V. Král, *Collect. Czech. Chem. Commun.* **2006**, *71*, 1278–1302.

- [9] In a nutshell, the mobility of gaseous ions can be compared to chromatography in the condensed phase. An electric field gradient serves as the mobile phase, which provides the driving force for the forward transport of the gaseous ions, and an inert gas (here: N<sub>2</sub> at about 2 mbar) serves as the stationary phase and provides a resistance against forward transport. For two isobaric ions of different shape (“potato and cigar”), the more compact one interacts less with the buffer gas and thus reaches the detector before the more extended ion of identical mass.
- [10] The experiments were performed with a SYNAPT G2 ion-mobility mass spectrometer (Waters, Manchester, UK). In brief, the instrument has an ESI source from which the ions are extracted towards a quadrupole mass filter (Q) for parent-ion selection. In the ion-mobility mode, the ions are first collected in an argon-filled linear ion trap (Trap) and then admitted in pulses through a helium cooling cell into the ion-mobility unit (IM) in which nitrogen is present at an approximate pressure of 2 mbar. Next, the ions pass a transfer cell (Trans) and enter the source region of a reflectron time-of-flight (TOF) mass spectrometer, which continuously records mass spectra with a mass resolution ( $m/\Delta m$ ) of approximately 25 000.
- [11] For recent reviews of ion-mobility measurements of gaseous ions, see: a) A. B. Kanu, P. Dwivedi, M. Tam, L. Matz, H. H. Hill, Jr., *J. Mass Spectrom.* **2007**, *43*, 1–22; b) B. C. Bohrer, S. I. Mererbloom, S. L. Koeniger, A. E. Hilderbrand, D. E. Clemmer, *Annu. Rev. Anal. Chem.* **2008**, *1*, 293–327; c) J. Puton, M. Nousiainen, M. Sillanpaa, *Talanta* **2008**, *76*, 978–987.
- [12] Aside from gravity, our IM-MS setup does not have any element of asymmetry. Thus, enantiomeric ions cannot be distinguished from each other. Such a separation can be achieved by addition of chiral dopants to the mobility unit, see: P. Dwivedi, C. Wu, L. M. Matz, B. H. Clowers, W. F. Siems, H. H. Hill, Jr., *Anal. Chem.* **2006**, *78*, 8200–8206.
- [13] For an ESI study on the mechanism of formation of Tröger bases, see: C. A. M. Abella, M. Benassi, L. S. Santos, M. N. Eberlin, F. Coelho, *J. Org. Chem.* **2007**, *72*, 4048–4054.
- [14] The arrival times in the SYNAPT G2 very much depend on the adjustments of the pressures and the voltage settings and can only be compared relative to each other. Also see: S. D. Pringle, K. Giles, J. L. Wildgoose, J. P. Williams, S. E. Slade, K. Thalassinios, R. H. Bateman, M. T. Bowers, J. H. Scrivens, *Int. J. Mass Spectrom.* **2007**, *261*, 1–12.
- [15] For a detailed consideration of the ESI process, see: W. D. Luedtke, U. Landman, Y.-H. Chiu, D. J. Levandier, R. A. Dressler, S. Sok, M. S. Gordon, *J. Phys. Chem. A* **2008**, *112*, 9628–9649.
- [16] J. B. Fenn, *Angew. Chem.* **2003**, *115*, 3999–4024; *Angew. Chem. Int. Ed.* **2003**, *42*, 3871–3894.
- [17] C. Trage, D. Schröder, H. Schwarz, *Chem. Eur. J.* **2005**, *11*, 619–627.
- [18] D. Schröder, M. C. Holthausen, H. Schwarz, *J. Phys. Chem. B* **2004**, *108*, 14407–14416.
- [19] D. Schröder, H. Schwarz, *Can. J. Chem.* **2005**, *83*, 1936–1940.
- [20] Other types of ESI sources do not apply a cone voltage, but most ESI sources have a device with a similar function to modify the ionization conditions.
- [21] For a recent example of probing the interconversion of different conformers using ion mobility, see: M. Grabenauer, T. Wyttenbach, N. Sanghera, S. E. Slade, T. J. T. Pinheiro, J. H. Scrivens, M. T. Bowers, *J. Am. Chem. Soc.* **2010**, *132*, 8816–8818.
- [22] Defined as  $x_{\text{frag}} = \sum_i I_{\text{frag},i} / (I_{\text{parent}} + \sum_i I_{\text{frag},i})$ , where  $I_i$  stands for the corresponding ion abundances. The difference between the two compounds is small but was observed reproducibly at five different collision energies.
- [23] The calculations were performed using the M06-2X density functional (Y. Zhao, D. G. Truhlar, *Theor. Chem. Acc.* **2008**, *120*, 215–241) in conjunction with 6-311++G(2df,2pd) basis sets. Energies refer to 0 K and include zero-point vibrational energy.
- [24] For both stereoisomers, protonation of the nitrogen atom bound to the central benzene ring is preferred (8.2 kJ mol<sup>−1</sup> for *syn*-1H<sup>+</sup> and 6.6 kJ mol<sup>−1</sup> for *anti*-1H) over that of the nitrogen bound to the outer naphthalene ring. Ring-protonated isomers are more than 100 kJ mol<sup>−1</sup> higher in energy.
- [25] For a recent example, see: L. Ducháčková, A. Kadlčíková, M. Kotora, J. Roithová, *J. Am. Chem. Soc.* **2010**, *132*, 12660–12667.
- [26] C. Adlhart, P. Chen, *Helv. Chim. Acta* **2000**, *83*, 2192–2196.
- [27] R. Imbihl, R. J. Behm, R. Schlögl, *Phys. Chem. Chem. Phys.* **2007**, *9*, 3459.